

## Tagging of RPS9 as a tool for ribosome purification and identification of ribosome-associated proteins

Bogdan Jovanovic<sup>1,2,3,4,\*</sup>, Lisa Schubert<sup>1,2,3,5</sup>, Fabian Poetz<sup>1,2,3</sup> and Georg Stoecklin<sup>1,2,3</sup>

<sup>1</sup>Mannheim Institute for Innate Immunoscience (MI3), Medical Faculty Mannheim, Heidelberg University, Mannheim, Germany

<sup>2</sup>Center for Molecular Biology of Heidelberg University (ZMBH), Heidelberg, Germany

<sup>3</sup>German Cancer Research Center (DKFZ) – ZMBH Alliance, Heidelberg, Germany

<sup>4</sup>Center for Human Molecular Genetics, Faculty of Biology, University of Belgrade, Belgrade, Serbia

<sup>5</sup>Novo Nordisks Foundation Center for Protein Research, University of Copenhagen, Copenhagen, Denmark

\*Corresponding author: bogdan.jovanovic@bio.bg.ac.rs

**Received:** December 5, 2020; **Revised:** December 28, 2020; **Accepted:** December 29, 2020; **Published online:** December 30, 2020

**Abstract:** Ribosomes, the catalytic machinery required for protein synthesis, are comprised of 4 ribosomal RNAs and about 80 ribosomal proteins in mammals. Ribosomes further interact with numerous associated factors that regulate their biogenesis and function. As mutations of ribosomal proteins and ribosome-associated proteins cause many diseases, it is important to develop tools by which ribosomes can be purified efficiently and with high specificity. Here, we designed a method to purify ribosomes from human cell lines by C-terminally tagging human RPS9, a protein of the small ribosomal subunit. The tag consists of a flag peptide and a streptavidin-binding peptide (SBP) separated by the tobacco etch virus (TEV) protease cleavage site. We demonstrate that RPS9-Flag-TEV-SBP (FTS) is efficiently incorporated into the ribosome without interfering with regular protein synthesis. Using HeLa-GFP-G3BP1 cells stably expressing RPS9-FTS or, as a negative control, mCherry-FTS, we show that complete ribosomes as well as numerous ribosome-associated proteins are efficiently and specifically purified following pull-down of RPS9-FTS using streptavidin beads. This tool will be helpful for the characterization of human ribosome heterogeneity, post-translational modifications of ribosomal proteins, and changes in ribosome-associated factors after exposing human cells to different stimuli and conditions.

**Keywords:** RPS9; ribosome-associated proteins; ribosome purification; streptavidin-binding peptide; affinity purification

## INTRODUCTION

The ribosome is a macromolecular complex that is required for one of the core biological processes – protein synthesis. Ribosomes are essential for all living organisms, and have become considerably larger during evolution [1]. The small 40S and the large 60S subunits of the mammalian ribosome together are comprised of four different ribosomal RNAs (rRNAs) and about 80 ribosomal proteins (RPs) [2]. Additionally, there are many ribosome-associated proteins (RAPs), collectively referred to as the ribo-interactome, which aid ribosome biogenesis and quality control, as well as translation regulation, specificity and fidelity. For example, listerin, an E3-ubiquitin ligase, associates

with the large ribosomal subunit and targets aberrant nascent polypeptides for proteasomal degradation [3]. Other well-known examples include the fragile-X-mental retardation protein (FMR1), which associates with polysomes and represses translation of a subset of mRNAs, and nucleophosmin (NPM1), a chaperone of ribosomal proteins [4,5]. Under stress conditions, when cellular defense mechanisms induce translation suppression, many cellular proteins interact with the small ribosomal subunit, either directly or indirectly, within cytoplasmic condensates called stress granules [6].

Mutations and malfunction of RPs lead to developmental abnormalities and many diseases, including Diamond-Blackfan anemia, Shwachman-Diamond

syndrome and X-linked dyskeratosis congenita [7]. Likewise, mutations and dysregulation of ribosome-associated proteins (RAPs) cause numerous diseases including different types of cancer [8,9]. Therefore, it is important to gain a detailed understanding of ribosome composition and the complex ribo-interactome. Recent studies revealed that ribosomes are heterogeneous, suggesting that ribosome subpopulations are dedicated to the translation of specific mRNAs [10-12]. Along with the composition of the ribosome and its interactome, posttranslational modifications (PTMs) play an important role in regulation of ribosome function. For example, under stress conditions small ribosomal subunits undergo prolyl hydroxylation at RPS23, which leads to altered translation of a subset of mRNAs [13].

In order to explore the mammalian ribo-interactome, ribosome heterogeneity and ribosomal PTMs, an efficient method for enrichment of RPs and RAPs is required. While several methods have been developed to this end, selective ribosome purification remains a challenge. Mass spectrometry of fractions after ultracentrifugation, enriched with in RPs and RAPs, as well as many non-related proteins, was performed [14], including similar work [2]. Affinity purification strategies proved to be more specific and were used in mouse models and mouse embryonic cells [15,16]. However, there is still no system for efficient affinity purification of ribosomes in human cell lines. One study tried to address this question by tagging RPS9 with HaloTag, but probably, due to the size of the tag, RPS9 was not efficiently incorporated into ribosomes, thus not allowing effective purification [17].

We have developed a new approach for purifying ribosomes and RAPs in human cell lines. A protein of the small ribosomal subunit, RPS9, was tagged with Flag-TEV-SBP, which allowed efficient pulldown of the ribosome and convenient detection of the RPS9 protein. Our system can be used in any human cell line, providing many options for its utilization and application.

## MATERIALS AND METHODS

### Cell culture

Human embryonic kidney cells, HEK293, HeLa and HeLa-GFP-G3BP1 [18] cells were cultured in Dulbecco's modified Eagle's medium (DMEM; Sigma-Aldrich, USA)

supplemented with 10% fetal bovine serum (Biochrom, UK), 2 mM L-glutamine, 100 U/mL penicillin and 0.1 mg/mL streptomycin (all PAN Biotech, Germany). Cells were grown at 37°C and 5% CO<sub>2</sub>.

### Plasmid cloning

For cloning of RPS9 into TOPuro-Flag-TEV-SBP, the cDNA of RPS9 was amplified from total RNA from HEK293 cells using MMLV RT (Promega, USA) for reverse transcription, followed by PCR amplification using Q5 DNA polymerase (NEB, USA) together with primers G3505 (5'-GAGGATCCCCACCATGCCAGTG-CCCCGAGCTGGG-3') and G3506 (5'-CTCTCGA-GATCCTCCTCCTCGTCGTCCTCC-3'), and the PCR product of 603 bp length was digested with BamHI and XhoI, and ligated into the BamHI and XhoI sites of TOPuro-Flag-TEV-SBP (p3373) using T4 DNA ligase and rapid ligase buffer (both from Fermentas, USA). The resulting plasmid TOPuro-RPS9-FTS (p3402) was verified by Sanger sequencing.

For cloning of pcDNA3-RPS9-FTS (p3438), TOPuro-RPS9-FTS (p3402) was digested with KpnI and BclI, and the 775-bp fragment containing RPS9-Flag-TEV-SBP was ligated into the KpnI and BamHI sites of pcDNA3 (p2000). The resulting plasmid pcDNA3-RPS9-FTS (p3438) was verified by Sanger sequencing.

To generate pcDNA3-mCherry-FTS (p3460), the Flag-TEV-SBP sequence was first cloned as a KpnI-BclI fragment from TOPuro-Flag-TEV-SBP (p3373) into the KpnI and BamHI sites of pcDNA3 (p2000), giving the pcDNA3-Flag-TEV-SBP plasmid. The mCherry sequence was isolated by BamHI digestion from pcDNA3-mCherry-CDK1r (p3454), and ligated into the BamHI site of pcDNA3-Flag-TEV-SBP. In pcDNA3-Flag-TEV-SBP, the stop-codon between mCherry and the FTS tag was removed via site-directed mutagenesis using primers G3795 (5'-GAG-GATCCACGCGTCCAGTGTGGTG-3') and G3796 (5'-TTCTCCCCCATGCAGGTC-3'). The resulting plasmid pcDNA3-mCherry-FTS (p3460) was verified by Sanger sequencing.

### Generation of stable cell lines

Cells (1.5 x 10<sup>5</sup>) were seeded in one well of a 6-well plate. After 24 h, HeLa-GFP-G3BP1 cells were transfected with

pcDNA3-RPS9-FTS (p3438) or pcDNA3-mCherry-FTS (p3460) using TurboFectin (Origene, USA) according to the manufacturer's manual. The next day, cells were split into two 15-cm dishes and selection was started by the addition of geneticin/G418 (Gibco, USA) at a final concentration of 400  $\mu\text{g}/\text{mL}$ . After 10 days of selection, a serial dilution of the mass culture was made to obtain single clones. On average, 0.5 cells were seeded per well in a 96-well plate. Once the clones had grown into larger colonies, they were transferred to 24-well plates and grown until confluency. Screening for RPS9-FTS-positive clones was performed by immunofluorescence microscopy using anti-Flag antibody in combination with fluorescence. Mass cultures of HeLa-GFP-G3BP1 cells transfected with mCherry-FTS were grown under selection pressure and subjected to fluorescence-activated cell sorting (FACS) to obtain a population of mCherry-FTS-positive cells.

### Immunofluorescence

Cells were seeded onto glass coverslips and left overnight. The following day, cells were fixed and permeabilized with ice-cold methanol for 3 min, washed with phosphate buffered saline (PBS) and blocked with 3% bovine serum albumin (BSA) in PBS for 1 h at room temperature. Coverslips were then incubated with rocking for 1 h at room temperature or overnight at 4°C with the primary antibody against Flag diluted in PBS containing 0.1% sodium azide. Cells were washed with PBS three times for 5 min before incubation for 1 h at room temperature with donkey anti-mouse Cy3-coupled secondary antibody (Jackson ImmunoResearch Laboratories, USA), diluted 1:1000 in PBS and Hoechst dye (1:10000, Sigma, USA). After washing again three times for 5 min, coverslips were mounted onto glass slides using a solution of 14% polyvinyl alcohol (P8136, Sigma) and 30% glycerol in PBS. Microscopy was performed on a Leica DM 5000 Microscope using a 20x or 40x dry objective.

### Streptavidin pull-down

HeLa GFP-G3BP1-RPS9-FTS and HeLa-GFP-G3BP1-mCherry-FTS cells were seeded in 15-cm dishes,  $3 \times 10^6$  cells per dish. After 24 h, cells pellets were collected and lysed in 750  $\mu\text{L}$  Nonidet-40 (NP-40) lysis buffer (150 mM NaCl, 1% NP-40, 50 mM Tris, 10% glycerol, 1

mM  $\text{MgCl}_2$ , 1 mM dithiothreitol (DTT)) supplemented with Complete Protease Inhibitor Cocktail (Roche, Switzerland). The samples were tumbled for 30 min at 4°C before the nuclei were removed by centrifugation for 10 min at 9000  $\times g$ . Thirty  $\mu\text{L}$  of the supernatant were taken as an input sample, and the remaining supernatant was incubated with 30  $\mu\text{L}$  prewashed streptavidin-Sepharose beads (GE Healthcare, USA) overnight at 4°C under gentle rotation. Next, the beads were washed 5 times on ice with 500  $\mu\text{L}$  NP-40 washing buffer (300 mM NaCl, 1% NP-40, 50 mM Tris, 10% glycerol, 1 mM  $\text{MgCl}_2$ , 1 mM DTT), and collected by centrifugation for 2 min at 400  $\times g$  and 4°C after each washing step. For elution, 32  $\mu\text{L}$  of biotin (50 mM) were added to the dry beads, and the samples were rotated for 1 h at 4°C. After centrifugation for 2 min at 400  $\times g$  and 4°C, the supernatant was transferred to a fresh tube, and 8  $\mu\text{L}$  of 5 $\times$  sample buffer were added. Finally, the samples were boiled for 10 min at 95°C and separated by sodium dodecyl sulfate (SDS)-polyacrylamide gel electrophoresis (PAGE) or stored at -20°C for later use.

### Western blot analysis

Protein samples were resolved on Tris-glycine polyacrylamide (5-20% gradient or 12%) gels and transferred to nitrocellulose membranes (0.2  $\mu\text{m}$  pore size, Peqlab, Germany). The membranes were blocked in 5% skimmed milk in PBS containing 0.1% sodium azide (PBS-A), incubated with primary antibodies diluted in PBS-A, and washed three times in a 150-mM NaCl solution containing 50 mM Tris, pH 7.5, 1% Tween-20. After washing, the membranes were incubated with horseradish peroxidase-coupled secondary antibodies (Jackson ImmunoResearch Laboratories, USA) diluted in PBS. Five additional washes were performed before adding Western Lightning enhanced chemiluminescence (ECL) substrate (PerkinElmer, USA) for detection. The following antibodies were used: mouse anti-Flag (F3165, Sigma, USA), rabbit anti-RPS9 (18215-1-AP, Proteintech, USA), goat anti-eIF3B (sc-16377, Santa Cruz, USA), rabbit anti-RPS6 (#2217, Cell Signaling, USA), mouse anti-RPS3 (sc-376098, Santa Cruz USA), rabbit anti-eIF4G (sc-11373, Santa Cruz USA), mouse anti-G3BP1 (sc-81940, Santa Cruz), rabbit anti-RPL7 (14583-1-AP, Proteintech USA), rabbit anti-NF- $\kappa$ B p65 (sc-109, Santa Cruz, USA).

## Polysome profile analysis

Cells were seeded onto 10-cm dishes one day before the experiment and kept subconfluent in order to prevent translation suppression by contact inhibition. Prior to lysis, cells were treated with 100  $\mu\text{g}/\text{mL}$  cycloheximide for 5 min at room temperature in order to stabilize polysomes. The cells were washed with ice-cold PBS, lysed on the dish by adding 200  $\mu\text{L}$  polysome lysis buffer (20 mM Tris HCl pH 7.5, 150 mM NaCl, 5 mM  $\text{MgCl}_2$ , 1 mM DTT, 100  $\mu\text{g}/\text{mL}$  cycloheximide, 1% Triton X-100, 40 U/mL RNasin<sup>TM</sup> (Thermo Fisher Scientific, USA), EDTA-free complete protease inhibitors (Roche, Switzerland) and harvested by scraping. Lysates were rotated for 10 min at 4°C and cleared by centrifugation at 9000  $\times g$  for 10 min at 4°C. Forty  $\mu\text{L}$  of lysate were saved for Western blot analysis before the cellular lysate was loaded onto linear, 17-50% sucrose gradient; sucrose was dissolved in 20 mM Tris-HCl, pH 7.5, 5 mM  $\text{MgCl}_2$ , 150 mM NaCl. Sucrose density gradient centrifugation was carried out at 35000 rpm at 4°C in a Beckman SW60 rotor for 2.5 h. Polysome profiles were recorded by measuring the absorbance at 254 nm using a Teledyne ISCO Foxy Jr. system and PeakTrak software. The profiles were manually aligned according to their 80S peaks using Microsoft Excel.

For Western blot analysis, thirteen 300- $\mu\text{L}$  fractions were collected during fractionation with Teledyne ISCO Foxy Jr. system. Then, 300  $\mu\text{L}$  Tris (20 mM, pH 7.5) together with 10  $\mu\text{L}$  StrataClean resin beads (Agilent, USA) were added to each fraction for protein recovery. The beads were rotated overnight at 4°C and centrifuged at 400  $\times g$  for 2 min. Following removal of the supernatant, protein was extracted from the beads by the addition of 30  $\mu\text{L}$  of 2 $\times$  SDS-sample buffer and boiling for 10 min at 95°C. Finally, the protein samples were separated by SDS-PAGE or stored at -20°C for later analysis.

## Protein mass spectrometry

Mass spectrometry was performed at the mass spectrometry core facility of the Center for Molecular Biology of Heidelberg University. Label-free quantification (LFQ) with MaxQuant software was used to determine the abundances of the detected peptides. For comparison between samples, LFQ values were normalized with the LFQ value of  $\beta$ -actin (ACTB). LFQ values of proteins not detected in one sample were set to 1.

## Statistical analysis

Statistical analysis and creation of graphics was performed using R and Microsoft Excel software. Statistical significance was calculated by performing Student's t-test.

## RESULTS

### Cells attenuate the expression of endogenous RPS9 when overexpressing RPS9-Flag-TEV-SBP

Our first goal was to generate a construct expressing a human RP of the 40S small ribosomal subunit to be used for the purification of 40S subunits or the whole ribosome. We chose to tag RPS9 at its C-terminus, as this position is on the surface of the small ribosomal subunit and should therefore be accessible to antibodies during immunoprecipitation procedures. Addition of large tags such as green fluorescent protein (GFP) can interfere with the structure of the ribosome or prevent tagged RP from incorporation into the ribosome. Therefore, we chose a small tag, Flag-TEV-SBP (FTS), which allows for easy detection and efficient immunoprecipitation. After cloning of the puromycin resistance-containing vector TOPpuro-RPS9-FTS, we used Western blot analysis to evaluate its expression in transiently transfected HeLa cells. RPS9-FTS was detected with anti-Flag antibody at the expected size of about 32 kDa (Fig. 1).

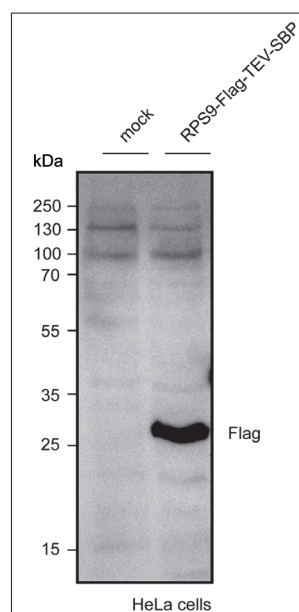


**Fig. 1.** Transient expression of RPS9-FTS in HeLa cells. HeLa cells were transfected with TOPpuro-RPS9-FTS, and cytoplasmic lysates were prepared after 24 h. Western blot analysis was carried out using an anti-Flag antibody.

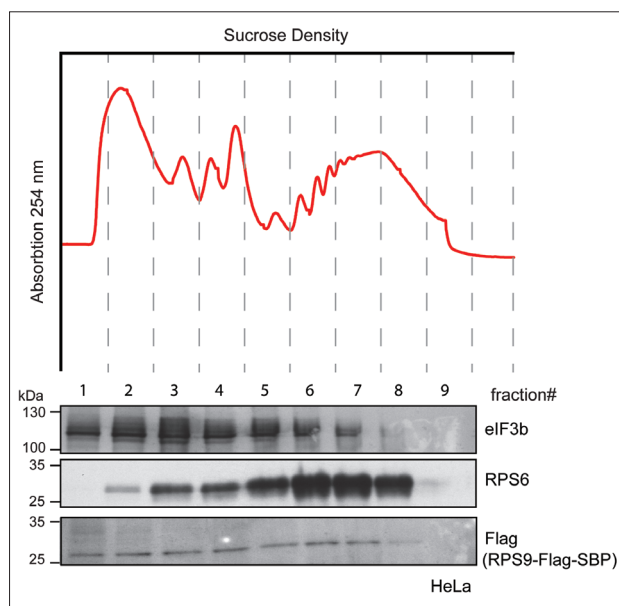


**Fig. 2.** Polysome profile analysis of HeLa cells transiently expressing RPS9-FTS. HeLa cells were transfected with TOPuro-RPS9-FTS, and cycloheximide was added to the cultures after 24 h immediately before preparing cytoplasmic lysates. Lysates were separated by sucrose density gradient centrifugation and analyzed by continuous UV (254 nm) absorption recording. Fractions were collected and subjected to Western blot analysis using antibodies against eIF3B and RPS6. Expression of RPS9-FTS was determined using anti-Flag antibody.

To determine if tagged RPS9 is incorporated into functional ribosomes, we used sucrose density gradient centrifugation to assess the overall translation rate of HeLa cells transiently transfected with TOPpuro-RPS9-FTS. As can be seen in Fig. 2, transient overexpression of RPS9-FTS did not perturb global translation, as the polysomal profiles appeared to be typical with about 77% of total ribosomes present in polysomes. Western blot analysis of fractions of the sucrose density gradient revealed that RPS9-FTS migrated in polysomes and monosomes, but also in the free fraction #1 (Fig. 2). The endogenous small ribosomal subunit protein RPS6 was enriched in polysomal fractions and absent from the free RNA fraction. Translation initiation factor eIF3b was enriched in the 40S fraction #3, similarly to previous observations [19].

### Generation of a stable cell line expressing RPS9-FTS

Transiently expressed RPS9-FTS was also found to be present in the ribosome-free fraction (Fig. 2), similar to a previous study where HA-tagged RPL22 was used

for ribosome purification in a mouse model [16]. This indicated that not all RPS9-FTS was incorporated into ribosomes in the transiently transfected cells, which is a potential problem. Therefore, our next goal was to generate a HeLa cell line stably expressing RPS9-FTS at a lower level, with better incorporation into ribosomes.

When cells are exposed to damage or unfavorable conditions, RPs of the 40S small subunit, including RPS9, separate together with many cytosolic proteins within stress granules by liquid-liquid phase separation [20]. We therefore chose to stably transfect RPS9-FTS in HeLa cells already expressing the stress granule (SG) marker protein GFP-G3BP1 [18], since immunoprecipitation of G3BP1 can be used for enrichment of SG components [21]. Since the HeLa-GFP-G3BP1 cell line is already resistant to puromycin, RPS9-FTS was cloned into a pcDNA3 vector, which confers resistance to geneticin/G418. Additionally, we generated mCherry-FTS as a negative control for the purification procedure, whereby RPS9-interacting proteins can be distinguished from those that associate with the Flag-TEV-SBP tag. After transfection of HeLa-GFP-G3BP1 cells with pcDNA3-RPS9-FTS and pcDNA3-mCherry-FTS, selection with G418, and subcloning by serial dilution, single clones were screened by immunofluorescence microscopy using an anti-Flag antibody. HeLa-GFP-G3BP1-RPS9-FTS clone #4 as well as the HeLa-GFP-G3BP1-mCherry-FTS mass culture were chosen for further analysis. Sucrose density gradient centrifugation analysis revealed that both stable cell lines, RPS9-FTS and mCherry-FTS, have normal polysomal profiles (Fig. 3A, B). Importantly, RPS9-FTS comigrated flawlessly with endogenous RPS9 in the polysomal fractions and was not detected in the free fraction (Fig. 3B), indicating that RPS9-FTS was fully incorporated into ribosomes. The analysis of cytoplasmic protein lysates confirmed that RPS9-FTS partially replaced endogenous RPS9, reducing its expression by about 30% (t-test,  $P < 0.001$ ) (Fig. 3C, D).

### Pull-down of RPS9-FTS purifies ribosomal proteins and ribosome-associated factors

We used the HeLa-GFP-G3BP1-RPS9-FTS cell line to optimize a ribosome pull-down approach for purifying RPs together with ribosome interactors. We performed SBP pull-down experiments using

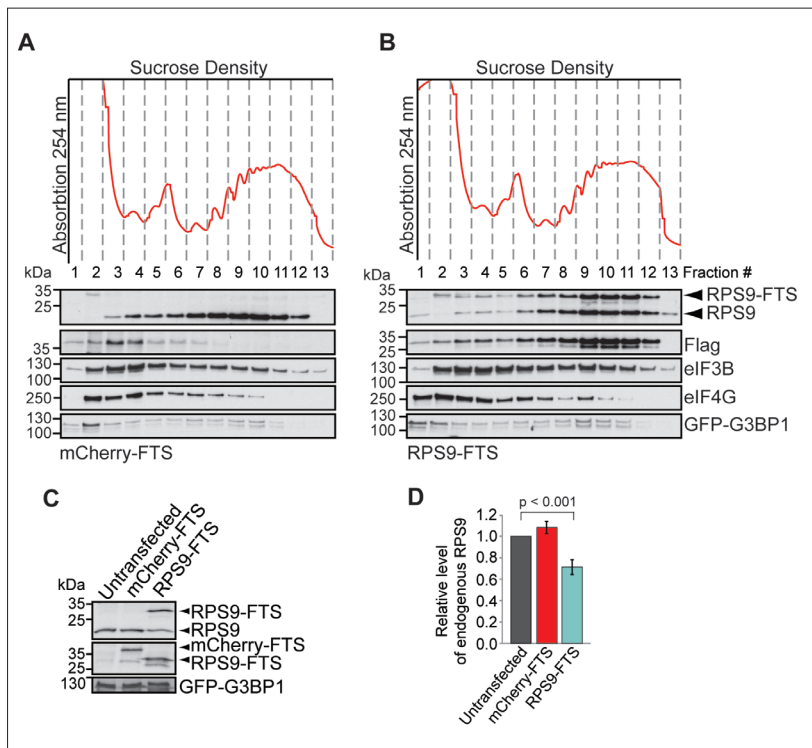


**Fig. 3.** Polysome profile analysis of HeLa-GFP-G3BP1 cells stably expressing mCherry-FTS or RPS9-FTS. **A** – Lysates of cycloheximide-treated HeLa-GFP-G3BP1-mCherry-FTS cells were separated by sucrose density gradient centrifugation and analyzed by continuous UV (254 nm) absorption recording. Fractions were collected and subjected to Western blot analysis using antibodies against RPS9, Flag, eIF3B, eIF4G and G3BP1. **B** – Analysis as in A from HeLa-GFP-G3BP1-RPS9-FTS cells. **C** – Expression levels of RPS9 in HeLa, HeLa-GFP-G3BP1-mCherry-FTS and HeLa-GFP-G3BP1-RPS9-FTS cells. **D** – Quantification of C; the graph shows mean values $\pm$ SD, n=3.

streptavidin-Sepharose beads. We observed that bound proteins could be eluted very efficiently by the addition of large amounts (50 mM) of biotin, even in the absence of SDS (Fig. 4A). The use of a native elution procedure reduced the amount of contaminating proteins in the eluate, and potentially allowed for the isolation of translation-competent ribosomes.

Cytosolic lysates from HeLa-GFP-G3BP1-mCherry-FTS and HeLa-GFP-G3BP1-RPS9-FTS cells were used for pull-down of the tagged proteins (Fig. 4B) and detection of specific isolation of RPL7, RPS6 and RPS3 in the RPS9-FTS eluate; NF- $\kappa$ B-p65, a protein without any association with the ribosome, was absent from both purifications (Fig. 4C).

When the same eluates were analyzed by mass spectrometry and quantified using MaxQuant software (Fig.5), 80 RPs were detected in the RPS9-FTS purification, 70 of which were enriched more than 2-fold

compared to the mCherry-FTS purification (Supplementary Table S1). This result implied successful pull-down of the entire ribosome by RPS9-FTS. In addition to RPs, 196 non-RPs were enriched more than 2-fold in the RPS9-FTS purification compared to the mCherry-FTS purification (Supplementary Table S2). When the non-ribosomal proteins were subjected to GO term analysis by Panther[22,23] and GOnet software [24], proteins could be sorted into more than 300 categories (Supplementary Table S3); the three broadest main protein categories found to be significantly overrepresented were as follows: rRNA processing proteins, spliceosomal components, translation factors and mRNA regulators. The list of non-ribosomal interacting proteins includes many nucleolar and cytosolic factors involved in ribosome biogenesis including BRIX1, EBNA1BP2, NCL, NOB1, NOC4L, NOL6, NOP14, NPM1, NPM3, NSA2, RIOK1, RIOK2, RIOK3, RRP7A, TSR1, WBSR22, indicating that RAPs were also isolated successfully by RPS9-FTS pull-down.

## DISCUSSION

Changes in the interactome and modifications of the ribosome are rapid regulatory mechanisms to alter translation rates when needed [12]. To explore such changes, reliable proteomics of isolated ribosomes is needed. Several studies in different model organisms, including mammalian systems, have used different approaches for ribosome isolation in order to identify means of translation regulation. Initial strategies made use of fractionation approaches, while later approaches attained higher specificity through affinity purification methods. Affinity purification of tagged ribosomes has been reported for various species, including *E. coli*, *D. melanogaster* and *S. cerevisiae*, showing that this approach allows successful isolation of ribosomes, associated proteins and mRNAs[25–27]. Endogenously

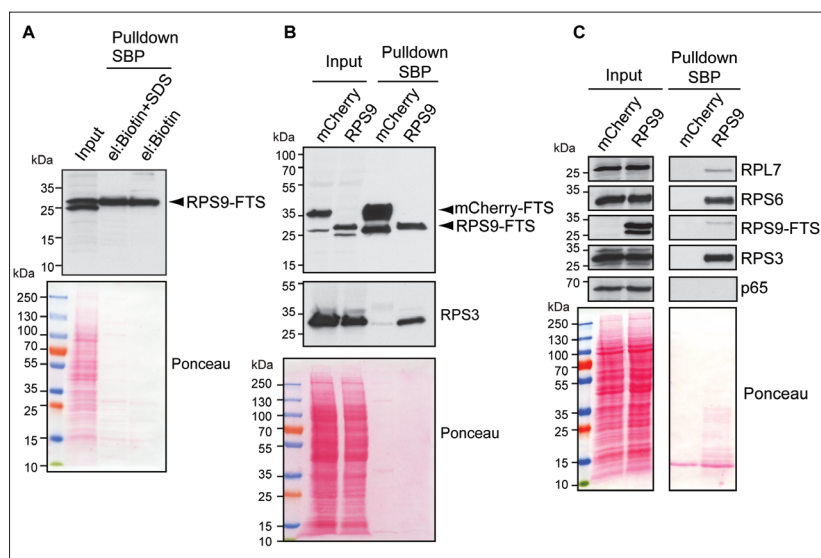


**Fig. 4.** Purification of ribosomal proteins via streptavidin pull-down of RPS9-FTS. **A** – Cytoplasmic lysates were prepared from RPS9-FTS cells and subjected to pull-down with streptavidin-Sepharose beads. Proteins were eluted by incubation with biotin (50 mM) or a combination of biotin and boiling in SDS-sample buffer. Samples were analyzed by Western blotting using anti-Flag antibody; the membrane was stained with Ponceau prior to blotting, electroelution. **B** – Streptavidin pull-down as in **A** was applied to mCherry-FTS and RPS9-FTS cells in parallel; biotin (50 mM) was used for elution. **C** – Streptavidin pull-down carried out as in **B**. Samples analyzed by Western blotting using antibodies against RPS9, RPS3, RPS6 and RPL7. Immunoblotting against NF- $\kappa$ B-p65 was used to show specificity of binding and elution.

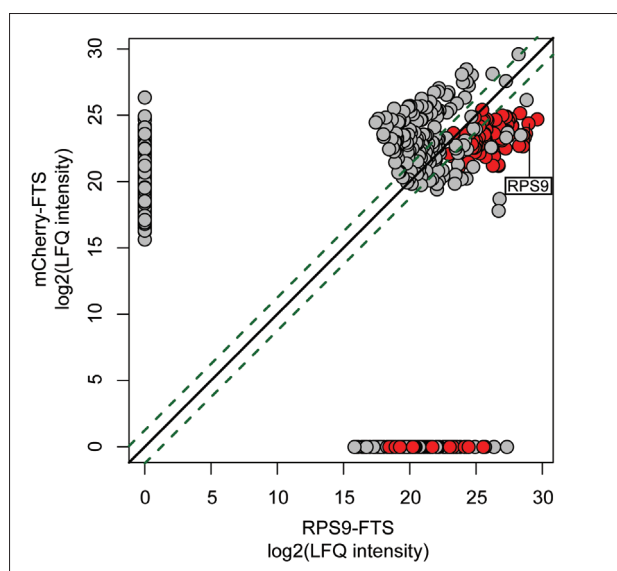


**Fig. 5.** Identification of proteins interacting with RPS9-FTS by mass spectrometry. **A** - HeLa-GFP-G3BP1-RPS9-FTS and control HeLa-GFP-G3BP1-mCherry-FTS cells were used for pull-down with streptavidin-Sepharose beads, and proteins were eluted by incubation with biotin (50 mM). Eluates were subjected to protein mass spectrometry and quantified using MaxQuant software. All proteins identified in the mCherry-FTS or RPS9-FTS pull-down are plotted in the graph; RPs are in red; the dark green dashed line represents a threshold for a 2-fold change;  $n=1$ .

tagged RPL22, RPL36 and RPS17 were used for ribosome purification in mouse models and mouse embryonic stem cells[15]. While tagging of RPL22 led to reduced incorporation into ribosomes, tagging of RPL36 and RPS17 overcame this problem. To our knowledge, no successful and efficient ribosome affinity purification approach has been reported for human cells to date, although research on this topic has been performed [17].

Herein, we developed a highly specific ribosome affinity purification approach for human cell lines. The establishment of such an approach is crucial for a better understanding of translation and its regulation in human cells under physiological and pathological conditions and upon exposure to different stimuli. RPS9-FTS has several advantages. It can be used for almost all human immortalized cell lines, which can

be efficiently transfected and therefore allow cell-type specific research on the ribosome and translation control mechanisms. When using these constructs with other cell lines, the transfection protocol has to be optimized for each cell line. The Flag-TEV-SBP tag allows for easy detection and immunoprecipitation via the Flag tag, efficient pull-down via streptavidin beads, and native elution using either Flag peptide or biotin or the TEV cleavage site. The stringency and purity of the pull-down could be further increased by tandem affinity purification using both streptavidin and Flag antibody. This could be of advantage for assays where the presence of RAPs should be minimal.

Pull-down of RPS9-FTS from stably transfected HeLa-GFP-G3BP1 cells allowed us to detect almost all RPs and many RAPs, as illustrated by the abundance of translation and ribosome biogenesis factors. Since spliceosomal proteins and mRNA processing factors were also among the identified proteins, it appears that mRNPs were isolated along with ribosomes. Introduction of a limited RNase digestion step prior to elution could help to separate RAPs from mRNPs.

When the list of RAPs identified in this study is compared to the human orthologs of mouse RAPs, identified by Simsek et al. [15], 94 significantly enriched RAPs are found to be in common. We could identify 138 proteins that were not found by Simsek et al., however, their dataset contained 419 RAPs that were not found in this study. The information about identified RAPs is solely based on mass spectrometry analysis and final conclusions about the ribo-interactome have to be further confirmed with other methods (e.g. immunoprecipitation and Western blotting) in both studies. One also has to consider that the comparison was conducted between different cell types and that each cell type has a specific set of RAPs. Nevertheless, both studies efficiently purified RPs and extended datasets with RAPs represent an excellent starting point for further research of the ribo-interactome.

Since HeLa-GFP-G3BP1-RPS9-FTS cells co-express tagged G3BP1, a core component of stress granules, this cell line can additionally be used for exploring RPs and RAPs within stress granules. Arsenite, a strong inducer of oxidative stress and stress granules, leads to O-linked  $\beta$ -N-acetylglucosamine (O-GlcNAc) modification of several ribosomal proteins; the O-GlcNAc modification was found to be essential for the assembly of stress granules [28]. In our dataset, OGFOD1, a prolyl-hydroxylase required for O-GlcNAc modification, was one of the 20 proteins related to stress granule assembly that were enriched after RPS9 pull-down (Supplementary Table S4). We anticipate that HeLa-GFP-G3BP1-RPS9-FTS cells will be helpful for further characterization of the ribo-interactome and ribosomal PTMs during stress granule assembly and upon exposure of cells to different stimuli.

To conclude, this study demonstrates that RPS9-FTS is an efficient and easy-to-use tool for the isolation of ribosomes and their associated factors under native conditions, and will be useful for research on translation control in human cells.

**Funding:** This work was supported by Grant SFB 1036 and TRR 186 from the Deutsche Forschungsgemeinschaft to GS.

**Acknowledgments:** We are grateful to Sergey Melnikov (Newcastle University, UK) for helping to select the ribosomal protein for tagging, and Katharina Hoerth (Medical Faculty Mannheim, University of Heidelberg, Germany) for providing HeLa-GFP-G3BP1 cells and useful advice. We also thank the Core Facility

for Mass Spectrometry and Proteomics (ZMBH, Heidelberg, Germany) for the mass spectrometry analysis, and Monika Langlotz (Flow Cytometry and FACS Core Facility (ZMBH, Heidelberg, Germany), for cell sorting.

**Author contributions:** BJ and LS contributed equally to the study. BJ and GS designed the study. BJ cloned the RPS9-Flag-TEV-SBP constructs, performed transient transfection experiments and together with LS, generated stable HeLa-GFP-G3BP1-RPS9-FTS cells. LS generated the HeLa-GFP-G3BP1-mCherry-FTS cell line and conducted most of the pull-down experiments. FP cloned the TOPpuro-Flag-TEV-SBP construct. All authors were involved in data analysis. BJ and GS wrote the manuscript with input from other authors.

**Conflict of interest disclosure:** The authors have declared that there is no conflict of interest.

## REFERENCES

1. Caetano-Anollés G, Caetano-Anollés D. Computing the origin and evolution of the ribosome from its structure - Uncovering processes of macromolecular accretion benefiting synthetic biology. *Comput Struct Biotechnol J*. 2015;13:427-47.
2. Belin S, Hacot S, Daudignon L, Therizols G, Pourpe S, Mertani HC, Rosa-Calatrava M, Diaz J. Purification of ribosomes from human cell lines. *Curr Protoc Cell Biol*. 2010;Chapter 3:Unit 3.40.
3. Joazeiro CAP. Mechanisms and functions of ribosome-associated protein quality control. *Nat Rev Mol Cell Biol*. 2019;20(6):368-83.
4. Darnell JC, Van Driesche SJ, Zhang C, Hung KYS, Mele A, Fraser CE, Stone EF, Chen C, Fak JJ, Chi SW, Licatalosi DD, Richter JD, Darnell RB. FMRP stalls ribosomal translocation on mRNAs linked to synaptic function and autism. *Cell*. 2011;146(2):247-61.
5. Drozd M, Delhay S, Maurin T, Castagnola S, Grossi M, Brau F, Jarjat M, Willemsen R, Capovilla M, Hukema RK, Lalli E, Bardoni B. Reduction of Fmr1 mRNA Levels Rescues Pathological Features in Cortical Neurons in a Model of FXTAS. *Mol Ther Nucleic Acids*. 2019;18:546-53.
6. Anderson P, Kedersha N, Ivanov P. Stress granules, P-bodies and cancer. *Biochim Biophys Acta*. 2015;1849(7):861-70.
7. Narla A, Ebert BL. Ribosomopathies: human disorders of ribosome dysfunction. *Blood*. 2010;115(16):3196-205.
8. Anczuków O, Krainer AR. Splicing-factor alterations in cancers. *RNA*. 2016;22(9):1285-301.
9. Israelsen WJ, Dayton TL, Davidson SM, Fiske BP, Hosios AM, Bellinger G, Li J, Yu Y, Sasaki M, Horner JW, Burga LN, Xie J, Jurczak MJ, DePinho RA, Clish CB, Jacks T, Kibbey RG, Wulf GM, Di Vizio D, Mills GB, Cantley LC, Vander Heiden MG. PKM2 isoform-specific deletion reveals a differential requirement for pyruvate kinase in tumor cells. *Cell*. 2013;155(2):397-409.
10. Li D, Wang J. Ribosome heterogeneity in stem cells and development. *J Cell Biol*. 2020;219(6): e202001108.
11. Ferretti MB, Karbstein K. Does functional specialization of ribosomes really exist? *RNA*. 2019;25(5):521-38.

12. Xue S, Barna M. Specialized ribosomes: a new frontier in gene regulation and organismal biology. *Nat Rev Mol Cell Biol.* 2012;13(6):355-69.
13. Singleton RS, Liu-Yi P, Formenti F, Ge W, Sekirnik R, Fischer R, Adam J, Pollard PJ, Wolf A, Thalhammer A, Loenarz C, Flashman E, Yamamoto A, Coleman ML, Kessler BM, Wappner P, Schofield CJ, Ratcliffe PJ, Cockman ME. OGFOD1 catalyzes prolyl hydroxylation of RPS23 and is involved in translation control and stress granule formation. *Proc Natl Acad Sci USA.* 2014;111(11):4031-6.
14. Reschke M, Clohessy JG, Seitzer N, Goldstein DP, Breitkopf SB, Schmolze DB, Ala U, Asara JM, Beck AH, Pandolfi PP. Characterization and Analysis of the Composition and Dynamics of the Mammalian Riboproteome. *Cell Reports.* 2013;4(6):1276-87.
15. Simsek D, Tiu GC, Flynn RA, Byeon GW, Leppek K, Xu AF, Chang HY, Barna M. The Mammalian Ribo-interactome Reveals Ribosome Functional Diversity and Heterogeneity. *Cell.* 2017;169(6):1051-65.e18.
16. Sanz E, Yang L, Su T, Morris DR, McKnight GS, Amieux PS. Cell-type-specific isolation of ribosome-associated mRNA from complex tissues. *Proc Natl Acad Sci U S A.* 2009;106(33):13939-44.
17. Gallo S, Beugnet A, Biffo S. Tagging of functional ribosomes in living cells by HaloTag® technology. *In Vitro Cell Dev Biol Animal.* 2011;47(2):132-8.
18. Haneke K, Schott J, Lindner D, Hollensen AK, Damgaard CK, Mongis C, Knop M, Palm W, Ruggieri A, Stoecklin G. CDK1 couples proliferation with protein synthesis. *J Cell Biol.* 2020;219(3):e201906147.
19. Hofmann S, Cherkasova V, Bankhead P, Bukau B, Stoecklin G. Translation suppression promotes stress granule formation and cell survival in response to cold shock. *Mol Biol Cell.* 2012;23(19):3786-800.
20. Banani SF, Lee HO, Hyman AA, Rosen MK. Biomolecular condensates: organizers of cellular biochemistry. *Nat Rev Mol Cell Biol.* 2017;18(5):285-98.
21. Jain S, Wheeler JR, Walters RW, Agrawal A, Barsic A, Parker R. ATPase-Modulated Stress Granules Contain a Diverse Proteome and Substructure. *Cell.* 2016;164(3):487-98.
22. Mi H, Muruganujan A, Thomas PD. PANTHER in 2013: modeling the evolution of gene function, and other gene attributes, in the context of phylogenetic trees. *Nucleic Acids Res.* 2013;41(Database issue):D377-386.
23. Thomas PD. PANTHER: A Library of Protein Families and Subfamilies Indexed by Function. *Genome Research.* 2003;13(9):2129-41.
24. Pomaznoy M, Ha B, Peters B. GONet: a tool for interactive Gene Ontology analysis. *BMC Bioinformatics.* 2018;19(1):470.
25. Ederth J, Mandava CS, Dasgupta S, Sanyal S. A single-step method for purification of active His-tagged ribosomes from a genetically engineered *Escherichia coli*. *Nucleic Acids Res.* 2009;37(2):e15.
26. Inada T, Winstall E, Tarun SZ, Yates JR, Schieltz D, Sachs AB. One-step affinity purification of the yeast ribosome and its associated proteins and mRNAs. *RNA.* 2002;8(7):948-58.
27. Thomas A, Lee P-J, Dalton JE, Nomie KJ, Stoica L, Costa-Mattioli M, Chang P, Nuzhdin S, Arbeitman MN, Dierick HA. A versatile method for cell-specific profiling of translated mRNAs in *Drosophila*. *PLoS One.* 2012;7(7):e40276.
28. Ohn T, Kedersha N, Hickman T, Tisdale S, Anderson P. A functional RNAi screen links O-GlcNAc modification of ribosomal proteins to stress granule and processing body assembly. *Nat Cell Biol.* 2008;10(10):1224-31.

### Supplementary Material

The Supplementary Material is available at: [http://serbiosoc.org.rs/NewUploads/Uploads/Jovanovic%20et%20al\\_Supplementary%20Material\\_6014.xlsx](http://serbiosoc.org.rs/NewUploads/Uploads/Jovanovic%20et%20al_Supplementary%20Material_6014.xlsx)